Supplementary Materials for "Coherent motions in confluent cell monolayer sheets"

Bo Li and Sean X. Sun

Department of Mechanical Engineering, Biomedical Engineering and Johns Hopkins Physical Sciences-Oncology Center, The Johns Hopkins University, Baltimore, Maryland 21218, USA

FORCES BETWEEN CELLS

To describe forces within an epithelial layer, a mathematical model must incorporate passive mechanical forces arising from cell shape elasticity and cell-cell adhesion, and active mechanical forces from cell protrusion and cell contraction. A standard model that incorporates passive cell mechanics as well as active cell contractility is the Dirichlet domain model of Honda (1). Here, cell mechanics is expressed in terms of a mechanical energy

$$E_i = \frac{1}{2} K_v (A_i - A_0)^2 - \gamma L_i + \Lambda L_i^m \qquad \text{(S1)}$$

where K_v , γ , and Λ are constants, A_i denotes the area (volume) of the i-th cell, and L_i is the circumferential length of the cell. In this model, the first term describes the cell elastically with a preferred area A_0 . The second term describes cell adhesion energy, which is related to bonds established by cadherins (2,3). The final term describes active contractility of the cell, which tends to minimize the cell circumferential length. m is a phenomenological parameter and typically it is taken to be 1 or 2. This model captures essential physics of cell-cell interaction, and has been successfully used to describe stationary cell morphology in epithelial sheets (2). Here we use this model as a starting point to consider cell motility in epithelial sheets.

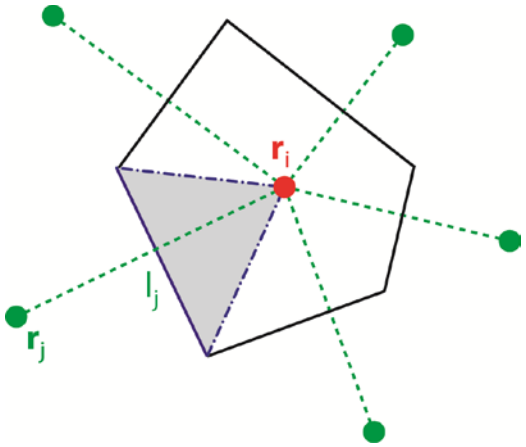

Figure S1: Cell geometry in our model. The interface between cells *i* and *j* is determined by the perpendicular bisector of the segment connecting points $\mathbf{r}_i$ and $\mathbf{r}_j$. The area of the cell is calculate by Eq. S2.

To introduce cell motility, it is necessary to consider the position of the *i*-th cell, $\mathbf{r}_i$ and write the mechanical energy in terms of it. However, Eq. (S1) cannot be easily written in terms of $\mathbf{r}_i$. Instead we introduce a slightly modified cell model. Using Dirichlet domains, the interface between two cells is still a straight line as in Eq. (S1), which is the perpendicular bisector of the segment connecting two neighboring points (Fig. S1). The area, A_i of each cell is the sum taken over the areas of sub-triangles, that is,

$$A_i = \frac{1}{4}\sum_{j=1}^{n_i} |\mathbf{r}_i - \mathbf{r}_j| \, l_j \tag{S2}$$

where l_j is the length of the interface between cell *i* and its neighbor cell *j*. n_i denotes the number of neighbors surrounding the *i*-th cell. For cell *i*, we write the mechanical energy (4)

$$E_i = \frac{1}{2}K_v(A_i - A_0)^2 + \frac{1}{2}K_s(\mathbf{r}_i - \mathbf{r}_{i0})^2 + \frac{1}{2}\sum_{j=1}^{n_i} K_c(\mathbf{r}_i - \mathbf{r}_j)^2 \tag{S3}$$

where K_v, K_s, and K_c are constants describing area elasticity, adhesion strength, and contractility, respectively. $\mathbf{r}_{i0}$ is the geometric center of the cell. First term is exactly the same as Eq. (S1). The second term also physically describes surface tension of the cell,

which tends to round up the cell. In 2D, the array of cells with minimal surface energy is the hexagonal lattice (4). In the case where the cell is completely symmetrical, $\mathbf{r}_i = \mathbf{r}_{i0}$, and this term is minimized. The last contractility term written in terms of $\mathbf{r}_i$ is different. However, it has a similar effects as the last term in Eq. (S1) because $L_i^2 = \left(\sum_{j=1}^{n_i} l_j\right)^2$ is closely correlated with $\sum_{j=1}^{n_i} (\mathbf{r}_i - \mathbf{r}_j)^2$, as shown in Fig. 2 in the main text. Therefore, Eq. (S3) is closely related to the Eq. (S1) for $m = 2$. If there is no cell motility, i.e., $\mathbf{F}_{i,p} = \mathbf{0}$, the system has a ground state, shown in the phase diagram in Fig. S2. We see that the phase diagram is similar to the phase diagram given by Eq. (S1) (2). The cell shape and area of three examples are illustrated in Fig. S3.

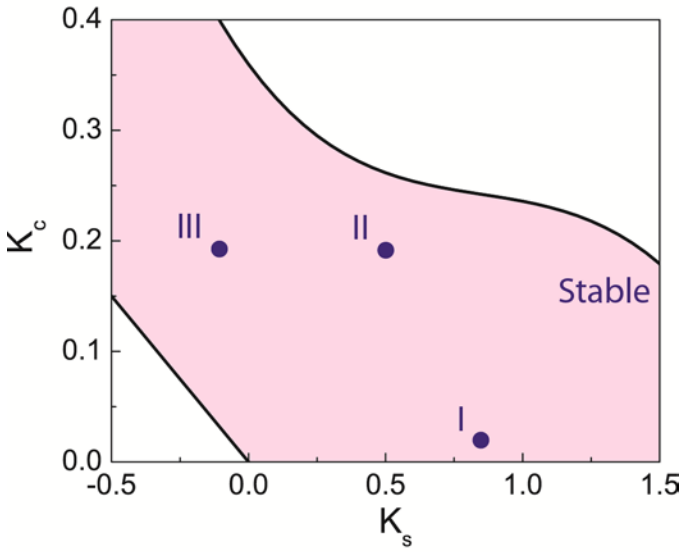

Figure S2: Phase Diagram of the cell monolayer at equilibrium from Eq. (S3). There exists a stable region in which the shape of cells is mostly hexagonal. Beyond this region, the cell shape is irregular and the area of cells may vanish. Three cases I, II, and III in the stable region are labeled and their shape and area characteristics are illustrated in Fig. S4. Cells also do not move without other forces.

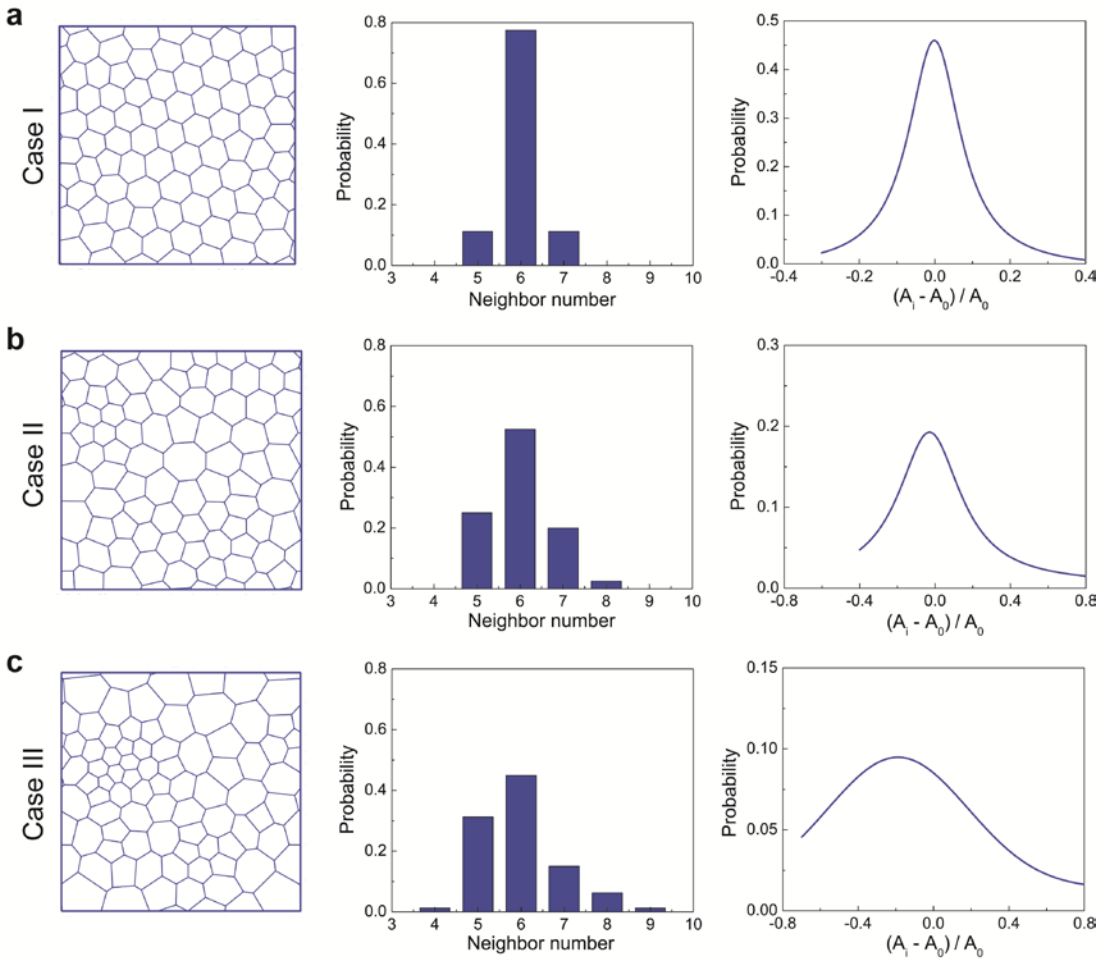

Figure S3: Shape, number of neighbors and area of cells in the stable region in Fig. S3. (a)-(c) Three cases I, II, and III labeled in Fig. S3.

From Eq. S3, the force on the *i*-th cell is

$$\mathbf{F}_i = -\frac{\partial E_i}{\partial \mathbf{r}_i} \tag{S4}$$

which gives an analytic expression of the form

$$\mathbf{F}_i = -\frac{K_v}{4}\sum_{j=1}^{n_i}\left[\frac{(\mathbf{r}_i-\mathbf{r}_j)l_i}{|\mathbf{r}_i-\mathbf{r}_j|}+|\mathbf{r}_i-\mathbf{r}_j|\frac{\partial l_i}{\partial \mathbf{r}_i}\right](A_i-A_0)-K_s(\mathbf{r}_i-\mathbf{r}_{i0})-\sum_{j=1}^{n_i}K_c(\mathbf{r}_i-\mathbf{r}_j) \tag{S5}$$

$\partial l_i/\partial \mathbf{r}_i$ can be expressed by $\mathbf{r}_i$ and the neighbors $\mathbf{r}_j$ but we omit it here since it is lengthy. During the simulations, it is found that the term $\partial l_i/\partial \mathbf{r}_i$ has small effect on the rotation frequency and cell shapes. So we ignore this term in the simulations. Without persistent

forces and random forces, cells do not move at steady state. To introduce motility, we introduce active protrusive forces and write the total force on cell *i* as

$$\mathbf{F}_i = \mathbf{F}_{i,p} + \mathbf{F}_{i,a} + \mathbf{F}_R \tag{S6}$$

where $\mathbf{F}_{i,p}$ is the passive force comprising of cell area elasticity and cell adhesion, which is described by the first two terms in Eq. (S5)

$$\mathbf{F}_{i,p} = -\frac{K_v}{4}\sum_{j=1}^{n_i}\left[\frac{(\mathbf{r}_i - \mathbf{r}_j)l_i}{|\mathbf{r}_i - \mathbf{r}_j|} + |\mathbf{r}_i - \mathbf{r}_j|\frac{\partial l_i}{\partial \mathbf{r}_i}\right](A_i - A_0) - K_s(\mathbf{r}_i - \mathbf{r}_{i0}) \tag{S7}$$

The active force $\mathbf{F}_{i,a}$ arises from directed cell protrusions and cell contractility (5,6)

$$\mathbf{F}_{i,a} = \alpha\frac{\int_{-\infty}^{t} e^{-\beta(t-\tau)}\mathbf{v}_i(\tau)\mathrm{d}\tau}{\left|\int_{-\infty}^{t} e^{-\beta(t-\tau)}\mathbf{v}_i(\tau)\mathrm{d}\tau\right|} - \sum_{j=1}^{n_i} K_c(t)(\mathbf{r}_i - \mathbf{r}_j) \tag{S8}$$

Note that here since the cell contractile force may vary with time K_c is also in principle a function of time.

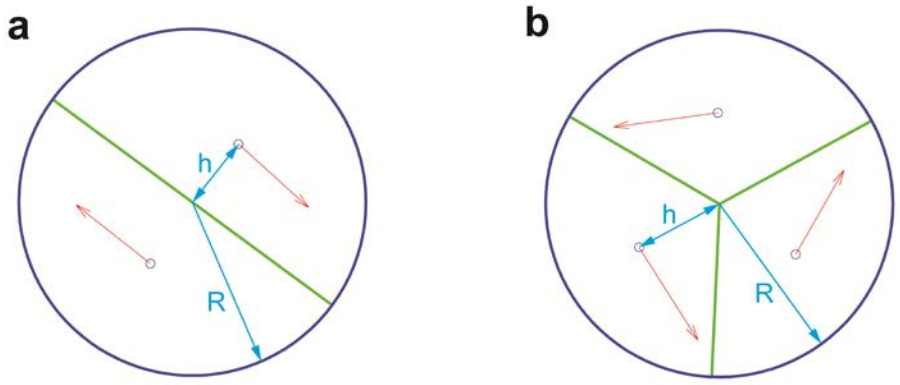

Figure S4: Two and three cell rotation on circular substrates. (a) Two cells rotating on a substrate. Here $h = 4R/(3\pi)$ when the system arrives at stable rotation. (b) Three cells rotating on a substrate. Here $h = \sqrt{3}R/\pi$ when the system arrives at stable rotation.

ROTATION OF TWO AND THREE CELLS

After initial equilibration, the system achieves a stable rotation as a rotating solid-disk (Fig. S4 and Movies S1 and S2). The cell center coincides with its geometric center which is at a distance h from center of the substrate with radius R.

ACTIVE TORQUE FOR CELL CLUSTER ON CIRCULAR SUBSTRATES

When the system rotate stably, the active force with short memory (large β) is approximately in the tangential direction. Therefore, we can calculate the active torque by (7)

$$T_\alpha \approx \alpha \int_0^R \frac{2\pi r^2}{A_0} \mathrm{d}r = \frac{2\pi\alpha R^3}{3A_0} \tag{S9}$$

The active torque T_α has to be balanced by the friction torque T_f (see Eq. (3) in main text) from the substrate. Using this, we obtain

$$\alpha \approx \frac{3}{4}\eta_s A_0 R\omega \tag{S10}$$

It indicates that in this case the relationship between α and ω is approximately linear. Rewrite Eq. S10 as $\omega R = 4\alpha/(3\eta_s A_0)$, which shows that the tangential velocity (ωR) of cells at the substrate edge is independent of the substrate size R (7).

MOVIES

Movie S1 Two cells rotating on a circular substrate.

Movie S2 Three cells rotating on a circular substrate.

Movie S3 Coherent cell rotation on a circular substrate with $N = 80$.

Movie S4 Coherent cell rotation on a circular substrate with $N = 200$.

Movie S5 Eccentric rotation in large system with $N = 500$.

Movie S6 Coherent rotation driven by a portion of cells with persistent force. The total number of cells in the system is $N = 50$.

Movie S7 Coherent cell rotation on a squared substrate with fixed boundary and $N = 80$.

Movie S8 Coherent cell rotation on a substrate with periodic boundary and $N = 80$.

SUPPORTING REFERENCES

1. Honda, H. 1978. Description of cellular patterns by Dirichlet domains: the two-dimensional case. J. Theor. Biol. 72: 523-543.
2. Farhadifar,R., J. -C. Röper, B. Aigouy, S. Eaton, and F. Jülicher. 2007. The influence of cell mechanics, cell-cell interactions, and proliferation of epithelial packing. Curr. Biol. 17: 2095-2104.
3. Marinari, E., A. Mehonic, S. Curran, J. Gale, T. Duke, and B. Baum, 2012. Live-cell delamination counterbalances epithelial growth to limit tissue overcrowding. Nature 484: 542-545.
4. Barrio, R. A., J. R. Romero-Arias, M. A. Noguez, E. Azpeitia, E. Ortiz-Gutiérrez, V. Hernández-Hernández, Y. Cortes-Poza, and E. R. Álvarez-Buylla. 2013. Cell patterns emerge from coupled chemical and physical fields with cell proliferation dynamics: the Arabidopsis thaliana root as a study system. PLoS Comput. Biol. 9: e1003026.
5. Selmeczi, D., S. Mosler, P. H. Hagedorn, N. B. Larsen, and H. Flyvbjerg. 2005. Cell motility as persistent random motion: theories from experiments. Biophys. J. 89: 912-931.
6. Kabla, A. J. 2012. Collective cell migration: leadership, invasion and segregation. J. R. Soc. Interface. 9: 3268-3278.
7. Doxzen, K., S. R. K. Vedula, M. C. Leong, H. Hirata, N. S. Gov, A. J. Kabla, B. Ladoux, and C. T. Lim. 2013. Guidance of collective cell migration by substrate geometry. Integr. Biol. 5: 1026-1035.